The Hurst phenomenon and fractional Gaussian noise made easy

DEMETRIS KOUTSOYIANNIS

Department of Water Resources, School of Civil Engineering, National Technical University of Athens, Heroon Polytechneiou 5, GR-157 80 Zographou, Greece

dk@hydro.ntua.gr

Abstract The Hurst phenomenon, which characterizes hydrological and other geophysical time series, is formulated and studied in an easy manner in terms of the variance and autocorrelation of a stochastic process on multiple temporal scales. In addition, a simple explanation of the Hurst phenomenon based on the fluctuation of a hydrological process upon different temporal scales is presented. The stochastic process that was devised to represent the Hurst phenomenon, i.e. the fractional Gaussian noise, is also studied on the same grounds. Based on its studied properties, three simple and fast methods to generate fractional Gaussian noise, or good approximations of it, are proposed.

Key words Hurst phenomenon; fractional Gaussian noise; persistence; climate change

Le phénomène de Hurst et le bruit fractionnel gaussien rendus faciles dans leur utilisation

Résumé On formule et étudie d'une manière simple le phénomène de Hurst, qui caractérise des séries chronologiques en hydrologie et en géophysique, en termes de variance et d'autocorrélation d'un processus stochastique considéré selon des échelles temporelles multiples. De plus, on présente une explication simple du phénomène de Hurst sur la base de la fluctuation d'un processus hydrologique dans des échelles temporelles multiples. On étudie également d'une manière analogue le bruit fractionnel gaussien qui constitue le processus stochastique construit pour représenter le phénomène de Hurst. En se basant sur les propriétés étudiées de ce processus, on propose trois méthodes simples et rapides pour générer du bruit fractionnel gaussien, voire une bonne approximation.

Mots clefs phénomène de Hurst; bruit fractionnel gaussien; persistance; changement climatique

INTRODUCTION

While investigating the discharge time series of the Nile River in the framework of the design of the Aswan High Dam, Hurst (1951) discovered a special behaviour of hydrological and other geophysical time series, which has become known as the "Hurst phenomenon". This behaviour is essentially the tendency of wet years to cluster into wet periods, or of dry years to cluster into drought periods. The term "Joseph effect" introduced by Mandelbrot (1977) has been used as an alternative for the same behaviour. Since its discovery, the Hurst phenomenon has been verified in several environmental quantities, such as wind power variations (Haslett & Raftery, 1989), global mean temperatures (Bloomfield, 1992), flows of the River Nile (Eltahir, 1996), flows of the River Warta, Poland (Radziejewski & Kundzewicz, 1997), monthly and daily inflows of Lake Maggiore, Italy (Montanari *et al.*, 1997), annual streamflow records across the continental United States (Vogel *et al.*, 1998), and indexes of North Atlantic Oscillation (Stephenson *et al.*, 2000). In addition, the Hurst phenomenon has gained new interest today due to its relationship to climate changes (e.g. Evans, 1996).

Several types of models, such as fractional Gaussian noise (FGN) models (Mandelbrot, 1965; Mandelbrot & Wallis, 1969a,b,c), fast fractional Gaussian noise models (Mandelbrot, 1971), broken line models (Ditlevsen, 1971; Mejia *et al*., 1972), fractional autoregressive integrated moving-average models (Hosking, 1981, 1984), and symmetric moving average models based on a generalized autocovariance structure (Koutsoyiannis, 2000), have been proposed to reproduce the Hurst phenomenon when generating synthetic time series (see also Bras & Rodriguez-Iturbe, 1985).

Although hydrologists may agree that the Hurst phenomenon is inherent to hydrological time series, generally they prefer to use other, more convenient models to generate synthetic hydrological time series, such as autoregressive (AR) models, moving average (MA) models, or combinations of the two (ARMA). For example, widespread stochastic hydrology packages, such as LAST (Lane & Frevert, 1990), SPIGOT (Grygier & Stedinger, 1990), and CSUPAC1 (Salas, 1993), have not implemented any of the above listed types of models that respect the Hurst phenomenon, but rather they use AR, MA and ARMA models, which cannot reproduce the Hurst phenomenon. It is known that this reproduction may be essential in reservoir studies, especially in reservoirs performing over-year regulation with draft close to the mean annual inflow (Bras & Rodriguez-Iturbe, 1985, p. 265).

There must be several reasons explaining this unwillingness to reproduce the Hurst phenomenon in hydrological practice. First, it is difficult to understand and explain, at least in comparison to typical statistical behaviour of everyday life processes. Stochastic hydrology texts (e.g. Yevjevich, 1972; Haan, 1977; Kottegoda, 1980; Bras & Rodriguez-Iturbe, 1985; Salas *et al*., 1980; Salas, 1993) adopt the original Hurst's mathematical formulation. This is in terms of the so-called rescaled range and, as shown in the Appendix, it involves complexity and estimation problems. In addition, the nature of the Hurst phenomenon has been the subject of debate, as discussed by Bras & Rodriguez-Iturbe (1985, p. 214). Second, the algorithms that are used to generate synthetic data series respecting the Hurst phenomenon are complicated. Third, the typical models of this category have several weak points such as narrow type of autocorrelation functions that they can preserve, and difficulties to preserve skewness and to perform in multivariate setting.

In contrast, this paper attempts to show that the Hurst phenomenon is essentially very simple to formulate, understand and reproduce in synthetic series—in some aspects much simpler than the typical AR processes, which, in addition, are not consistent with long historical hydroclimatic records. A mathematical formulation is offered, based on the relationship of the process variance with the temporal scale of the process. In addition, a simple explanation of the Hurst phenomenon is offered, based on the fluctuation of a hydrological process at different time scales. Three original simple methods are provided to generate fractional Gaussian noise or good approximations of it. Throughout this paper, use of the range concept is totally avoided. To explain the reasons for this and also to link with the existing approaches of the Hurst phenomenon, the Appendix is devoted to range-related topics.

The presentation of all issues is made as simple as possible throughout, because the purpose of the paper is *not* to review the state of the art of the research related to the Hurst phenomenon, *nor* to give the complete mathematical details of it (for the latter see the comprehensive monograph by Beran, 1994), but rather (a) to assemble an easy-to-understand mathematical basis and physical explanation of the phenomenon

and (b) to provide means for an easy implementation (e.g. using a spreadsheet package) of the methods, both for estimation and simulation.

MULTIPLE TIME-SCALE PROPERTIES OF TYPICAL STOCHASTIC PROCESSES

Hydrological processes such as rainfall, runoff, evaporation, etc. are often modelled as stationary stochastic processes in discrete time. Let such a process be denoted as X_i with $i = 1, 2, \ldots$, denoting discrete time (e.g. years). Further, let its mean be $\mu = E[X_i]$, its autocovariance $\gamma_j = \text{cov}[X_i, X_{i+j}]$ and its autocorrelation $\rho_j = \text{corr}[X_i, X_{i+j}] = \gamma_j/\gamma_0$ ($j = 0, \pm 1, \pm 2, \ldots$).

In fact, i represents the continuous time interval $[(i-1)\delta, i\delta]$ where δ is the time scale of interest. Very often, several scales that are integer multiples of a basic time scale δ are of interest. For example, when investigating the firm yield of a reservoir that performs over-year regulation, the basic time scale could be one year, but time scales of several years are also of interest. Similarly, in short-scale rainfall modelling the basic time scale could be 5 or 10 min, but time scales of several hours are of interest, too. Let $k\delta$ be a time scale larger than δ where k is a positive integer (for convenience δ will be omitted and time scale k referred to). The aggregated stochastic process on that time scale is denoted as $Z_i^{(k)}$:

$$Z_i^{(k)} := \sum_{l=(i-1)k+1}^{ik} X_l \tag{1}$$

Obviously, for $k = 1$, $Z_i^{(1)} = X_i$; for $k = 2$, $Z_1^{(2)} = X_1 + X_2$, $Z_2^{(2)} = X_3 + X_4$, etc. The statistical properties of $Z_i^{(k)}$ can be derived from those of X_i. For example, the mean is:

$$E\left[Z_i^{(k)}\right] = k\mu \tag{2}$$

whilst the variance and autocovariance (or autocorrelation) can be found by:

$$\gamma_j^{(k)} = \text{cov}\left[Z_i^{(k)}, Z_{i+j}^{(k)}\right] = \sum_{l=1}^{k} \sum_{m=j\cdot k+1}^{(j+1)k} \gamma_{m-l} \qquad j = 0, \pm 1, \pm 2, \ldots \tag{3}$$

The autocovariance is related to the power spectrum of the process, which in the general case is the discrete Fourier transform (DFT; also termed the inverse finite Fourier transform) of γ_j, i.e.:

$$s_\gamma^{(k)}(\omega) := 2\gamma_0^{(k)} + 4\sum_{j=1}^{\infty} \gamma_j^{(k)} \cos(2\pi j\omega) = 2\sum_{j=-\infty}^{\infty} \gamma_j^{(k)} \cos(2\pi j\omega) \tag{4}$$

It is assumed in equation (4) that the frequency ω is in the interval $[0, 1/2]$, so γ_j is determined in terms of $s_\gamma(\omega)$ by the finite Fourier transform:

$$\gamma_j^{(k)} = \int_0^{1/2} s_\gamma^{(k)}(\omega) \cos(2\pi j\omega) d\omega \tag{5}$$

Before studying the process known as fractional Gaussian noise (FGN), which respects the Hurst phenomenon, two of the simplest stochastic models will be referred to. The first is the white noise, in which different X_i are independent identically

distributed random variables, so that $\gamma_j = 0$ (and $\rho_j = 0$) for $j \neq 0$. Then, the aggregated process has variance:

$$\gamma_0^{(k)} := \mathrm{var}\big[Z_i^{(k)}\big] = k\gamma_0 \tag{6}$$

autocovariance $\gamma_j^{(k)} = 0$, autocorrelation $\rho_j^{(k)} = 0$, and power spectrum independent of the frequency ω:

$$s_\gamma^{(k)}(\omega) = 2\gamma_0^{(k)} \tag{7}$$

As a second example, the simplest possible process with some memory, i.e. dependence of the current value on previous ones, is assumed. This is the AR(1) process and the dependence in the basic time scale is expressed by:

$$X_i = \rho X_{i-1} + V_i \tag{8}$$

where ρ is the lag-one autocorrelation coefficient ($-1 < \rho < 1$) and V_i ($i = 1, 2, \ldots$) are independent, identically distributed, random variables with mean $(1 - \rho)\mu$ and variance $(1 - \rho^2)\gamma_0$. The process is Markovian because the dependence of the current variable X_i on the previous variable X_{i-1} suffices to express completely the dependence of the present on the past. The autocorrelation of X_i is:

$$\rho_j := \mathrm{corr}\big[X_i, X_{i+j}\big] = \rho^{|j|} \tag{9}$$

Combining equations (9) and (3) and carrying out algebraic manipulations, it can be found that the aggregated process has variance:

$$\gamma_0^{(k)} = \gamma_0 \frac{k(1-\rho^2) - 2\rho(1-\rho^k)}{(1-\rho)^2}, \; \gamma_j^{(k)} = \gamma_0 \frac{\rho^{kj-k+1}(1-\rho^k)^2}{(1-\rho)^2} \qquad j \geq 1 \tag{10}$$

and autocorrelation:

$$\rho_1^{(k)} = \frac{\rho(1-\rho^k)^2}{k(1-\rho^2) - 2\rho(1-\rho^k)}, \; \rho_j^{(k)} = \rho_1^{(k)}\rho^{k(j-1)} \qquad j \geq 1 \tag{11}$$

By comparing equation (11) with equation (9) one may conclude that $Z_i^{(k)}$ is no longer a Markovian process but a more complicated one (in fact equation (11) corresponds to an ARMA(1,1) process; Box *et al.*, 1994, p. 81). In other words, the simple AR(1) process is an AR(1) process only on its basic time scale, whereas it becomes more complicated on aggregated time scales.

The power spectrum of the aggregated process $Z_i^{(k)}$ can be found by adapting the power spectrum of the AR(1) process (Box *et al.*, 1994, p. 58). After algebraic manipulations one obtains:

$$s_\gamma^{(k)}(\omega)/\gamma_0^{(k)} = 2 + 4\rho_1^{(k)} \frac{\cos(2\pi\omega) - \rho^k}{1 + \rho^{2k} - 2\rho^k \cos(2\pi\omega)} \tag{12}$$

For relatively small k, this gives a characteristic inverse S-shaped power spectrum that corresponds to a short memory process.

For a large aggregated time scale k, the numerator of equation (10) is dominated by the first term and the variance of the aggregated process becomes:

$$\gamma_0^{(k)} \approx k\frac{1+\rho}{1-\rho}\gamma_0 \tag{13}$$

i.e. it becomes proportional to the time scale k, similarly as in the white noise process. Also, from equation (11) one may observe that $\rho_1^{(k)}$ becomes small, as does $\rho_j^{(k)}$. Consequently, from equation (12) one concludes that the power spectrum becomes $s_\gamma^{(k)}(\omega) = \gamma_0^{(k)}$. Thus, if the process of interest is Markovian on the basic time scale, it tends to white noise for progressively increasing time scales. (In fact, this happens with higher order AR and ARMA processes as well.)

SOME REAL-WORLD EXAMPLES

Empirical evidence suggests that long historical hydroclimatic series may exhibit a behaviour very different from that implied by simple models such as those described above. To demonstrate this, two real-world examples are used. The first is the most intensively studied series, which also led to the discovery of the Hurst phenomenon (Hurst, 1951): the series of the annual minimum water level of the Nile River for the years 622–1284 AD (663 observations), measured at the Roda Nilometer near Cairo (Toussoun, 1925; Beran, 1994). The data are available from http://lib.stat.cmu.edu/S/beran. The second example is an even longer record: the series of standardized tree-ring widths from a palaeoclimatology study at Mammoth Creek, Utah, for the years 0–1989 (1990 values; year 0 in fact stands for 1 BC, as the calendar does not contain year 0). The data, originated from pine trees at elevation 2590 m, latitude 37°39′N, longitude 112°40′W (Graybill, 1990), are available from:
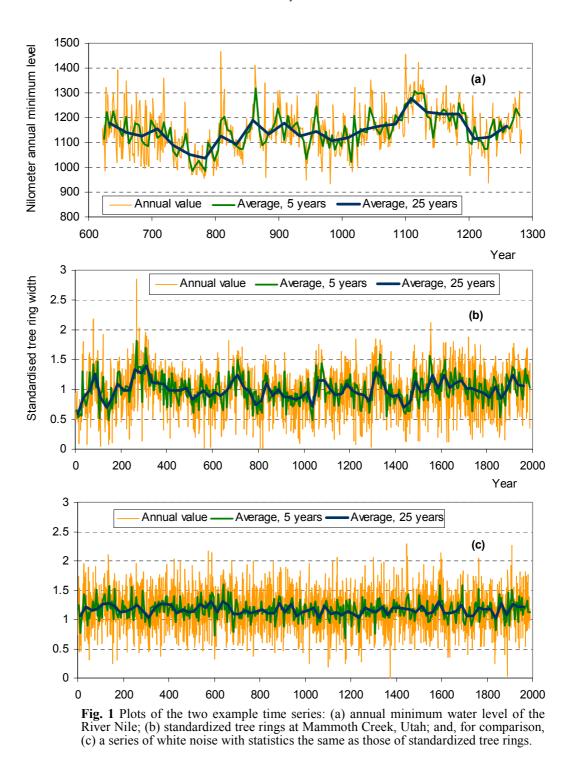ftp://ftp.ngdc.noaa.gov/paleo /treering/chronologies/asciifiles/usawest/ut509.crn.

In Fig. 1 the data values are plotted *vs* time for both example data sets. In addition, the 5-year and 25-year averages are shown, which represent the aggregated processes at time scales $k = 5$ and 25, respectively. For comparison, a series of white noise with statistics identical to those of standardized tree rings is also shown. It is observed that fluctuations of the aggregated processes, especially for $k = 25$, are much greater in the real-world time series than in the white noise series. These fluctuations could be taken as nonstationarities, that is, deterministic rising or falling trends that last 100–200 or more years. For example, if one had available only the data of the period 700–800 of either of the two time series, one would refer to it as a deterministic falling trend. However, the complete pictures for both series suggest that this is part of a large-scale random fluctuation rather than a deterministic trend.
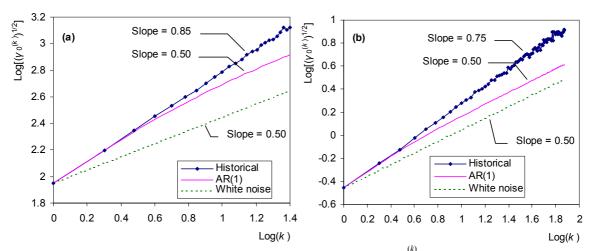
Figure 2 shows the standard deviation of the aggregated processes *vs* time scale k for the two example data sets (logarithmic diagrams). For comparison theoretical curves for the white noise and AR(1) models (equations (6) and (10), respectively) are also shown. Clearly, the plots of both series are almost straight lines on the logarithmic diagram with slopes 0.75–0.85. Both the white noise and the AR(1) models result in a slope equal to 0.5, significantly departing from the historical data.

Furthermore, Fig. 3 shows the autocorrelation coefficients of the aggregated processes for lag one and two, plotted *vs* the time scale k, for the example data sets. For comparison, theoretical curves for the AR(1) model are also plotted. The empirical autocorrelation coefficients are almost constant for all time scales, whereas AR(1) results in autocorrelations that drop down to zero for large time scales.
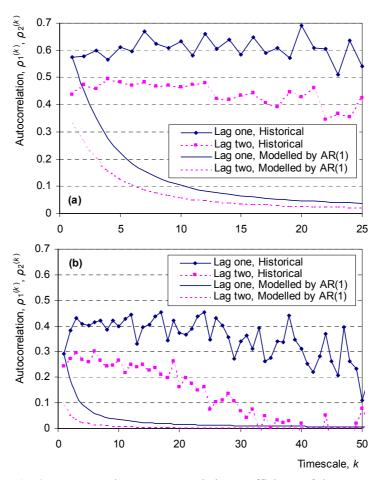
Finally, in Fig. 4, the autocorrelation functions of the example time series on the basic (annual) time scale are plotted along with the theoretical curves of the AR(1)

Fig. 1 Plots of the two example time series: (a) annual minimum water level of the River Nile; (b) standardized tree rings at Mammoth Creek, Utah; and, for comparison, (c) a series of white noise with statistics the same as those of standardized tree rings.
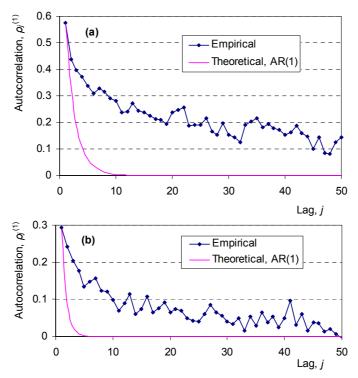
model. Clearly, the curves of AR(1) vanish off for lags 4–10, whereas the curves of the historical series are fat-tailed and do not vanish for lags as high as 50. In conclusion, this discussion provides some further evidence, using a multiple-time scale approach, to the well-known fact that the AR(1) model is inconsistent with hydroclimatic reality (a similar conclusion can be drawn for more complex processes of the ARMA type).

Fig. 2 Standard deviation of the aggregated processes $Z_i^{(k)}$ *vs* time scale k (logarithmic plots) for the two example data sets: (a) annual minimum water level of the River Nile; and (b) standardized tree rings at Mammoth Creek, Utah. For comparison theoretical curves for the white noise and AR(1) models are also shown.

Fig. 3 Lag-one and -two autocorrelation coefficients of the aggregated processes $Z_i^{(k)}$ *vs* time scale k for the two example data sets: (a) annual minimum water level of the River Nile; and (b) standardized tree rings at Mammoth Creek, Utah. For comparison the theoretical curves of the AR(1) model are also plotted.

Fig. 4 Autocorrelation functions of the two example time series on the basic (annual) scale: (a) annual minimum water level of the River Nile; and (b) standardized tree rings at Mammoth Creek, Utah. For comparison the theoretical curves of the AR(1) model are also plotted.

THE FRACTIONAL GAUSSIAN NOISE PROCESS

To restore consistency with reality, Mandelbrot (1965) introduced the process known as fractional Gaussian noise (FGN). Fractional Gaussian noise can be defined in discrete time (which is the scope here) in a manner similar to that used in continuous time (e.g. Saupe, 1988, p. 82). Specifically, FGN can be defined as a process satisfying the condition:

$$\left(Z_i^{(k)} - k\mu\right) \overset{\mathrm{d}}{=} \left(\frac{k}{l}\right)^{H} \left(Z_j^{(l)} - l\mu\right) \tag{14}$$

where the symbol $\overset{\mathrm{d}}{=}$ stands for equality in (finite-dimensional joint) distribution and H is a positive constant $(0 < H < 1)$ known as the Hurst exponent (or coefficient). Equation (14) is valid for any integer i and j (that is, the process is stationary) and any time scales k and l. As a consequence, for $i = j = l = 1$ one obtains:

$$\gamma_0^{(k)} = k^{2H}\gamma_0 \tag{15}$$

Thus, the standard deviation is a power law of k with exponent H, which agrees with the observation on the real-world cases described above. The extremely simple equation (15) can serve as the basis for estimating H (Montanari *et al.*, 1997).

It is easy then to show that, for any aggregated time scale k, the autocovariance function is independent of k, i.e. (Koutsoyiannis, 2002):

$$\rho_j^{(k)} = \rho_j = (1/2)\left[(j+1)^{2H} + (j-1)^{2H}\right] - j^{2H} \qquad j > 0 \tag{16}$$

again agreeing with the observation in the previous section. Apart from small j, this function is very well approximated by:

$$\rho_j^{(k)} = \rho_j = H(2H - 1)j^{2H-2} \tag{17}$$

which shows that autocorrelation is a power function of lag.

Notably, equation (16) can be obtained from a continuous time process $\Xi(t)$ with autocorrelation $\text{cov}[\Xi(t), \Xi(t + \tau)] = a\tau^{2H-2}$ (with constant $a = H(2H - 1)\gamma_0$), by discretizing the process using time intervals of any length δ and taking as X_i the average of $\Xi(t)$ in the interval $[(i - 1)\delta, i\delta]$. This enables an approximate calculation of the power spectrum of the process as:

$$s_\gamma^{(k)}(\omega) = 2\sum_{j=-\infty}^{\infty} \gamma_j^{(k)} \cos(2\pi j\omega) \approx 4\int_0^{\infty} a\tau^{2H-2}\cos(2\pi\tau\omega)\mathrm{d}\tau \tag{18}$$

which results in the approximation $s_\gamma^{(k)}(\omega) \approx a'\omega^{1-2H}$. To find the constant a' so as to preserve exactly the process variance γ_0, equation (5) is used to obtain $\gamma_0^{(k)} = a'/[(2 - 2H)2^{2-2H}]$, and, finally:

$$s_\gamma^{(k)}(\omega) \approx 4(1 - H)\gamma_0^{(k)}(2\omega)^{1-2H} \tag{19}$$

which is a power law of the frequency ω.

Similarly to AR(1), which uses one parameter ρ to express the correlation structure, FGN also uses one parameter, the Hurst exponent H. Therefore, one can characterize FGN as a simplified model of reality, noting that it is much more effective in representing hydroclimatic series than AR(1). A generalized and comprehensive family of processes, which can have a larger number of parameters and incorporates both FGN and ARMA processes, has been introduced by Koutsoyiannis (2000).

Comparing FGN to AR(1) in terms of basic statistical properties on multiple time scales, one may observe that the former is simpler than the latter. Thus, the expression of the process variance on any scale k (equation (15)) is much simpler that that of AR(1) (equation (10)). Similarly, the expression of autocorrelation on any scale k (equations (16)–(17)) is simpler that that of AR(1) (equation (11)).

A PHYSICAL EXPLANATION

A white noise process, e.g. a sequence of outcomes of consecutive throws of dice, is a very familiar concept. Under the assumption of a stable climate, the maximum flood peaks of consecutive years may be regarded as a white noise process as well, as there is no dependence between flood events in different hydrological years. Processes that have some memory are less familiar, but a Markovian (e.g. AR(1)) process is not difficult to explain. For example, Yevjevich (1972, p. 27) explained that the annual flow series is dependent and follows a Markovian process. To show this, he assumed that the catchment is stimulated by an effective precipitation process being white noise and that the water carry-over from year to year is ruled by a groundwater recession curve expressed as an exponential function of time.
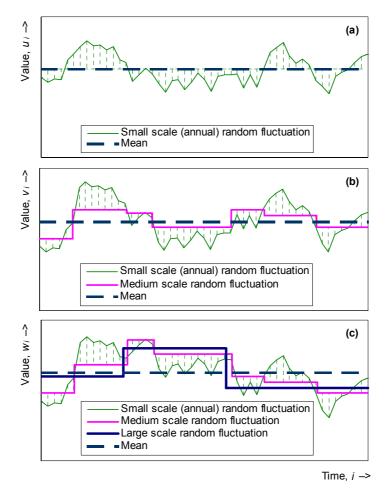
The Hurst phenomenon and the related FGN process are more difficult to understand. Mesa & Poveda (1993) classify the Hurst phenomenon as one of the most important unsolved problems in hydrology and state that "something quite dramatic must be happening from a physical point of view". FGN is very different from a Markovian process in that it implies a fat-tailed autocorrelation function. For instance, if the Hurst exponent is 0.85, as in the Nile example, then the autocorrelation for lag 100 (years) is as high as 0.15, whereas if the process were Markovian the autocorrelation would be practically zero even for lags 10 times less. Does the explanation of this behaviour of natural systems, such as the Nile water level or the Mammoth Creek tree-ring widths, rest on the self-organized criticality principle (e.g. Bak, 1996), i.e. a cooperative behaviour, where the different items of large systems act together in some concerted way? Or, does it rest on monotonic deterministic trends (Bhattacharya *et al.*, 1983), which can explain this behaviour mathematically? Or, is there any natural mechanism inducing a long memory to the system, which is responsible for the high autocorrelation for a lag of 100 years or more?

The author's explanation is much simpler and relies upon an "absence of memory" concept rather than a "long-term memory" concept. That is, the hypothesis is proposed that not only does the system "disremember" what was the value of the process 100 years (or more) ago, but it further "forgets" what the process mean at that time was. This explanation is consistence with the assertion of the National Research Council (1991) that climate "changes irregularly, for unknown reasons, on all timescales". The idea of irregular sporadic changes in the mean of the process appeared also in Salas & Boes (1980), but not in connection with FGN and not in the setting of multiple time scales. The idea of composite random processes with two time scales of fluctuation appeared in Vanmarcke (1983). For more mathematical explanations of FGN, the reader is referred to Beran (1994, pp. 14–20).

To demonstrate the proposed explanation, a Markovian process U_i is initially assumed (see Fig. 5(a)), with mean $\mu = E[U_i]$, variance γ_0 and lag-one autocorrelation coefficient $\rho = 0.20$. The autocorrelation function (given by equation (9)) for lags up to 1000 is shown in Fig. 6(a) along with the autocorrelation function for the FGN process with the same lag-one autocorrelation coefficient (0.20). One may observe the large difference of the two autocorrelation functions: that of the Markovian process practically vanishes off at lag four whereas that of FGN has positive values for lags as high as 100.

Now, a second process V_i is constructed by subtracting from the process U_i its mean $E[U_i] = \mu$ and superimposing the result to a new random process M that has again mean μ and some variance var[M] (see explanatory sketch on Fig. 5(b)). From a practical point of view, V_i could be considered similar to U_i but with time varying mean M. For the latter it is assumed that (a) any realization m of M lasts N years and is independent from previous realizations, and (b) N is a random variable exponentially distributed with mean λ. (This means that N can take non-integer values.) In other words, M takes a value $m_{(1)}$ that lasts n_1 years, then it changes to a value $m_{(2)}$ that lasts n_2 years, etc. (where the values $m_{(1)}, m_{(2)}, \ldots$ can be generated from any distribution). The exponential distribution of N indicates that the points of change are random points in time (Papoulis, 1991). If M_i denotes the instance of the M process at discrete time i (or continuous time $i\delta$), it can be shown that M_i is also Markovian with lag-one autocorrelation $\varphi = e^{-\delta/\lambda}$. The process V_i can be expressed in terms of U_i and M_i as:

Fig. 5 Illustrative sketch for multiple time scale random fluctuations of a process that can explain the Hurst phenomenon: (a) a time series from a Markovian process with constant mean; (b) the same time series superimposed to a randomly fluctuating mean on a medium time scale; and (c) the same time series further superimposed to a randomly fluctuating mean on a large time scale.
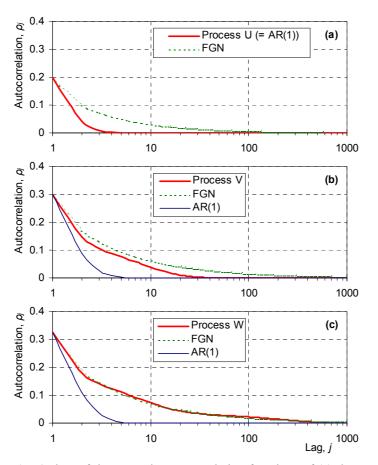
$$V_i = U_i + M_i - \mu \tag{20}$$

For a conceptualization of V_i one can consider the simpler case that M_i is a deterministic component, rather than a random process, with known value m_i at any time i, in which case $V_i = U_i + m_i - \mu$. Then V_i would be identical in distribution with U_i except that its mean would be m_i rather than μ. That is, V_i would be nonstationary with a time-varying mean m_i and all other moments constant in time. Returning to the initial assumption that M_i is a random process, one may infer from equation (20) that, since V_i is the sum of two stationary processes (U_i and M_i), it is itself a stationary process with mean μ.

It can be easily shown from equation (20) that the autocorrelation of V_i for lag j is:

$$\mathrm{corr}[V_i, V_{i+j}] = (1 - c)\rho^j + c\varphi^j \tag{21}$$

where $c := \mathrm{var}[M_i]/(\mathrm{var}[M_i] + \mathrm{var}[U_i])$. Setting, for instance, $\lambda = 7.5$ years and $c = 0.146$, one obtains the autocorrelation function shown in Fig. 6(b), which has departed from the AR(1) autocorrelation and approached the FGN autocorrelation.

Fig. 6 Plots of the example autocorrelation functions of (a) the Markovian process *U* with constant mean; (b) the process *U* superimposed to a randomly fluctuating mean on a medium time scale (process *V*); and (c) the process *V* further superimposed to a randomly fluctuating mean on a large time scale (process *W*). The superposition of fluctuating means increases the lag-one autocorrelation (from $\rho_1 = 0.20$ for *U* to $\rho_1 = 0.30$ and 0.33 for *V* and *W*, respectively) and also shifts the autocorrelation function from the AR(1) shape (also plotted in all three panels) towards the FGN shape (also shown in all three panels).

Further, one may take another step to construct a third process W_i by subtracting from the process V_i its mean $E[V_i] = \mu$ and superimposing the result to a new random process P with mean μ again (see explanatory sketch on Fig. 5(c)). Similar assumptions are made as in the previous step denoting by v the mean time between changes of the value of P and setting $\xi = e^{-\delta/v}$. The resulting composite process is:

$$W_i = V_i + P_i - \mu = U_i + M_i + P_i - 2\mu \tag{22}$$

Working as in the previous step one finds:

$$\text{corr}[W_i, W_{i+j}] = (1 - c_1 - c_2)\rho^j + c_1\varphi^j + c_2\xi^j \tag{23}$$

where c_1 and c_2 are positive constants (with $c_1 + c_2 < 1$). Setting, for instance, $\lambda = 7.5$ years, $v = 200$ years, $c_1 = 0.146$ and $c_2 = 0.036$, one obtains the autocorrelation function shown in Fig. 6(c), which has now become almost indistinguishable from the FGN autocorrelation for time lags from 1 to 1000.

This example illustrates that a Markovian underlying process can result in a process very similar to FGN if random fluctuations of the process mean occur on two different scales (e.g. 7.5 and 200 years), yet the resulting composite process being stationary. If one considers that fluctuations occur on a greater number of time scales, the degree of approximation of the composite process to the FGN process will be even better and can cover time lags greater than 1000 (although such lags may not be of practical interest in hydrology). In conclusion, the *irregular* changes of climate, that according to National Research Council (1991, p. 21) occur on all time scales, can be responsible for, and explain, the Hurst phenomenon.

In the above example, the process U, which represents the random fluctuations on the finest time scale, was considered as taking different values at each time step, whereas processes M and P, which represent random fluctuations on an intermediate and a large time scale, may have the same value for several time steps. This assumption was done for the sake of a simpler demonstration and indeed one could assume that M and P take different values at each time step, provided that their covariance structure remains Markovian with the same autocorrelation.

The above explanation may seem similar (from a practical point of view) to that by Klemeš (1974), who attributed the Hurst phenomenon to nonstationary means. However, there is a fundamental difference here. As shown in the above analysis, it was not assumed that means are nonstationary, but rather, that they are randomly varying on several scales. Nonstationarity of the mean would be the case if there existed a deterministic function expressing the mean as a function of time. In some hydrological texts (e.g. Kottegoda, 1980, p. 26), falling or rising trends, traced in hydrological time series, have been characterized as "deterministic components" and expressed as, say, linear functions of time; such a characterization would be justified if it were conditioned by a physical explanation and predictability, which has not been the case. Therefore, these trends should be more consistently regarded as large-scale random fluctuations. For example, (as already discussed above) the 25-year moving averages on the time series of Fig. 1 indicate that there exist falling and rising trends that follow an irregular random pattern rather than a regular deterministic one.

The conclusion of the above demonstration is that the nonstationarity notion is not necessary to explain the Hurst phenomenon. A stationary process can capture the Hurst effect and this agrees with Mandelbrot's notion. However, the explanation given herein is contrary to the concept of long memory; the high autocorrelations appearing for high lags do not indicate long memory, but are a consequence of the multi-scale random fluctuations as demonstrated with this simple example.

SIMPLE ALGORITHMS TO GENERATE FRACTIONAL GAUSSIAN NOISE

As discussed in the introduction, several algorithms have been proposed to generate time series that respect the Hurst phenomenon. For some of these, the source code is widely available (e.g. the Splus programs by Beran, 1994). However, some of the known algorithms are not so simple, either in understanding or implementation. In the following, three much simpler algorithms are proposed that can be applied even in a spreadsheet environment. These are based on the properties of FGN discussed above and can be used to provide approximations of FGN being adequate for practical hydrological purposes. In principle, all three algorithms can be tuned to become as

accurate as demanded. However, emphasis is given here to simplicity rather than accuracy. Although two of the algorithms work for any value of the Hurst exponent H in the interval (0, 1), all three have been tested on the subinterval (0.5, 1), which corresponds to the Hurst phenomenon (when $H < 0.5$ the autocorrelation function becomes negative for any lag, a case that is not met in hydrological practice).

A multiple time-scale fluctuation approach

In the previous section it was shown that the weighted sum of three exponential functions of the time lag (equation (23)) can give an acceptable approximation of the FGN autocorrelation function on the basic time scale. This observation leads to a (rather "quick and dirty") algorithm to generate FGN. An extensive numerical investigation showed that the values of parameters ρ, φ, and ξ that appear in equation (23), which provide the best (in terms of mean square error) approximation of equation (16), are given by the following:

$$\rho = 1.52(H - 0.5)^{1.32}, \quad \varphi = 0.953 - 7.69(1 - H)^{3.85},$$

$$\xi = \begin{cases} 0.932 + 0.087H & H \le 0.76 \\ 0.993 + 0.007H & H > 0.76 \end{cases} \tag{24}$$

The remaining parameters, c_1 and c_2, can be estimated such that the approximate autocorrelation function (equation (23)) matches the exact function (equation (16)) for two lags, e.g. lags 1 and 100. (Their values are obtained by solving two linear equations.) Comparison plots of approximate autocorrelation functions based on equations (23) and (24) *vs* the exact autocorrelation functions of FGN for various values of the Hurst exponent H are shown in Fig. 7.

In the previous section it was also shown how a process could be synthesized with the autocorrelation function (equation (23)) by assuming random changes of the mean on two time scales. However, there is a simpler way to utilize equation (23) for generation of a time series. Specifically, equation (23) represents the sum of three
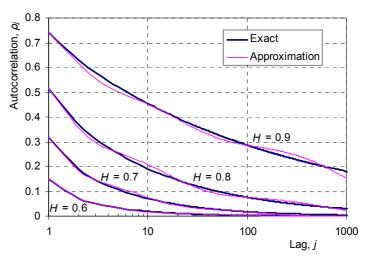

Fig. 7 Approximate autocorrelation functions based on equations (23) and (24) *vs* the exact autocorrelation functions of FGN for various values of the Hurst exponent H.
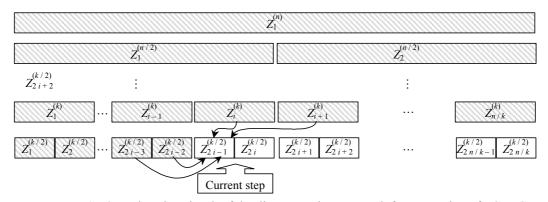
independent AR(1) processes like that in equation (8), with lag one correlation coefficients ρ, φ, and ξ, and variances $(1 - c_1 - c_2)\gamma_0$, $c_1\gamma_0$, and $c_2\gamma_0$, respectively.

It must be mentioned that this algorithm is based essentially on the same principle as the fast fractional Gaussian noise (FFGN) algorithm (Mandelbrot, 1971); the differences are that it uses only three AR(1) components, much less than the FFGN, and the parameters of the algorithm are determined by the much simpler equation (24). Although the achieved approximation with the three AR(1) components is sufficient in practice for lags as high as 1000, it can be improved by increasing the number of the AR(1) components to four, five, etc. However, equation (24) will be not applicable then and the variances and lag-one autocorrelations of the components must be estimated by minimizing the mean-squared departure of the composite autocorrelation function from that of the FGN process.

A disaggregation approach

The simple expressions of the statistics of the aggregated FGN process make possible a disaggregation approach for generating FGN. Here it is assumed that the desired length n of the synthetic series to be generated is 2^m, where m is an integer; if not, one can increase n to the next power of 2 and then discard the redundant generated items. First, the single value of $Z_1^{(n)}$ is generated knowing its variance $n^{2H}\gamma_0$ (from equation (15)). Then $Z_1^{(n)}$ is disaggregated into two variables on the time scale $n/2$, i.e. $Z_1^{(n/2)}$ and $Z_2^{(n/2)}$ and this process is continued until the series $Z_1^{(1)} \equiv X_1$, ..., $Z_n^{(1)} \equiv X_n$ is generated (see explanatory sketch on Fig. 8).

The proposed disaggregation algorithm is similar to the midpoint displacement method (Saupe, 1988, p. 84), but is more accurate. It is based on a disaggregation technique introduced by Koutsoyiannis (2001). Since it is an induction technique it suffices to describe one step. Assume that the generation on the time scale $k \leq n$ has been completed and the time series is being generated on the next time scale $k/2$ (see Fig. 8). Consider the generation step in which the higher-level amount $Z_i^{(k)}$ ($1 < i < n/k$) is disaggregated into two lower-level amounts $Z_{2i-1}^{(k/2)}$ and $Z_{2i}^{(k/2)}$ such that:

Fig. 8 Explanation sketch of the disaggregation approach for generation of FGN. Grey boxes indicate random variables whose values have been already generated prior to the current step and arrows indicate the links to those of the generated variables that are considered in the current generation step.

$$Z^{(k/2)}_{2i-1} + Z^{(k/2)}_{2i} = Z^{(k)}_i \tag{25}$$

Thus, it suffices to generate $Z^{(k/2)}_{2i-1}$ and then obtain $Z^{(k/2)}_{2i}$ from equation (25). At this generation step, the already generated values of previous lower-level time steps, i.e. $Z^{(k/2)}_1, \ldots, Z^{(k/2)}_{2i-2}$ and of the next higher-level time steps, i.e. $Z^{(k)}_{i+1}, \ldots, Z^{(k)}_{n/k}$ are available (see explanatory sketch on Fig. 8). Theoretically, it is necessary to preserve the correlations of $Z^{(k/2)}_{2i-1}$ with all previous lower-level variables and all next higher-level variables. However, one can obtain a very good approximation if one considers correlations with only one higher-level time step behind and one ahead. Under this simplification, $Z^{(k/2)}_{2i-1}$ can be generated from the linear relationship:

$$Z^{(k/2)}_{2i-1} = a_2 Z^{(k/2)}_{2i-3} + a_1 Z^{(k/2)}_{2i-2} + b_0 Z^{(k)}_i + b_1 Z^{(k)}_{i+1} + V \tag{26}$$

where a_2, a_1, b_0 and b_1 are parameters to be estimated and V is innovation whose variance has to be estimated, too. All unknown parameters can be estimated in terms of correlations of the form $\mathrm{corr}[Z^{(k/2)}_{2i-1}, Z^{(k/2)}_{2i-1+j}] = \rho_j$ where ρ_j is given by equation (16). Specifically, applying the methodology by Koutsoyiannis (2001) one finds:

$$\begin{bmatrix} a_2 \\ a_1 \\ b_0 \\ b_1 \end{bmatrix} = \begin{bmatrix} 1 & \rho_1 & \rho_2+\rho_3 & \rho_4+\rho_5 \\ \rho_1 & 1 & \rho_1+\rho_2 & \rho_3+\rho_4 \\ \rho_2+\rho_3 & \rho_1+\rho_2 & 2(1+\rho_1) & \rho_1+2\rho_2+\rho_3 \\ \rho_4+\rho_5 & \rho_3+\rho_4 & \rho_1+2\rho_2+\rho_3 & 2(1+\rho_1) \end{bmatrix}^{-1} \begin{bmatrix} \rho_2 \\ \rho_1 \\ 1+\rho_1 \\ \rho_2+\rho_3 \end{bmatrix} \tag{27}$$

and

$$\mathrm{var}[V] = \gamma^{(k/2)}_0 \left(1 - [\rho_2, \rho_1, 1+\rho_1, \rho_2+\rho_3][a_1, a_2, b_0, b_1]^T \right) \tag{28}$$

where the superscript T denotes the transpose of a vector.

All parameters are independent of i and k and therefore they can be used in all steps. When $i = 1$, the first two rows and columns of the above matrix and vectors are eliminated. Similarly, when $i = n/k$, the last row and column of the above matrix and vectors are eliminated. The sequences of previous and past variables that are considered for generating each lower-level variable, and the related parameters, can be directly expanded, to increase the accuracy of the method. However, this minimal configuration of the method gives satisfactory results.

A symmetric moving average approach

Koutsoyiannis (2000) introduced the so-called symmetric moving average (SMA) generating scheme that can be used to generate any kind of stochastic process with any autocorrelation structure or power spectrum. Like the conventional (backward) moving average (MA) process, the SMA scheme transforms a white noise sequence V_i into a process with autocorrelation by taking the weighted average of a number of V_i. In the SMA process, the weights a_j are symmetrical about a centre (a_0) that corresponds to the variable V_i, i.e.:

$$X_i = \sum_{j=-q}^{q} a_{|j|} V_{i+j} = a_q V_{i-q} + \ldots + a_1 V_{i-1} + a_0 V_i + a_1 V_{i+1} + \ldots + a_q V_{i+q} \tag{29}$$

where q theoretically is infinity but in practice can be restricted to a finite number, as the sequence of weights a_j tends to zero for increasing j. Koutsoyiannis (2000) also showed that the discrete Fourier transform $s_a(\omega)$ of the a_j sequence is related to the power spectrum of the process $s_\gamma(\omega)$ by:

$$s_a(\omega) = \sqrt{2s_\gamma(\omega)} \tag{30}$$

This enables the direct calculation of $s_a(\omega)$, which in the case of FGN, given equation (19), will be:

$$s_a(\omega) \approx 2\sqrt{(2-2H)\gamma_0}(2\omega)^{0.5-H} \tag{31}$$

Comparing equations (19) and (31) one may observe that $s_a(\omega)$ is approximately equal to the power spectrum of another FGN process with Hurst exponent $H' = (H + 0.5)/2$ and variance a_0 shown in equation (32). Consequently, one can use equation (16) to approximate the inverse Fourier transform of $s_a(\omega)$, i.e. the sequence of a_j itself:

$$a_0 = \frac{\sqrt{(2-2H)\gamma_0}}{1.5-H}, \quad a_j \approx \frac{a_0}{2}\left[(j+1)^{H+0.5} + (j-1)^{H+0.5} - 2j^{H+0.5}\right] \quad j > 0 \tag{32}$$

In conclusion, the generation scheme (equation (29)) with coefficients a_j determined from equation (32) can lead to a very easy algorithm for generating FGN. This method can also preserve the process skewness ξ_X by appropriately choosing the skewness of the white noise ξ_V. The relevant equations for the statistics of V_i, which are direct consequences of equation (29), are:

$$\left(a_0 + 2\sum_{j=1}^{s} a_j\right)E[V_i] = \mu, \quad \mathrm{var}[V_i] = 1, \quad \left(a_0^3 + 2\sum_{j=1}^{q} a_j^3\right)\xi_V = \xi_X \gamma_0^{3/2} \tag{33}$$

There are $q + 1$ weights a_j, so the model can preserve the first $q + 1$ terms of the autocovariance γ_j of the process X_i. Thus, the number q must be chosen at least equal to the desired number of autocorrelation coefficients m that are to be preserved. In addition, the ignored terms a_j beyond a_q must not exceed an acceptable tolerance βa_0. These two conditions in combination with equations (17) and (32) result in:

$$q \geq \max\left[m, \left(\frac{H^2 - 0.25}{2\beta}\right)^{1/(1.5-H)}\right] \tag{34}$$

The number q can be very high (thousands to hundreds of thousands) if H is large (e.g. >0.9) and β is small (e.g. <0.001). Approximate autocorrelation functions for lags up to 10 000 based on equations (29) and (32) *vs* the exact FGN autocorrelation functions for various values of H and q are shown in Fig. 9.

The accuracy of the method depends on q. However, even when $q \to \infty$ the method does not become exact because of the approximate character of equation (32). Although more accurate estimates of the a_j series can be obtained numerically by a method by Koutsoyiannis (2000), the estimates given by equation (32) are sufficiently accurate for practice. This is verified in Fig. 9 where theoretical and approximate autocorrelation functions are almost indistinguishable.
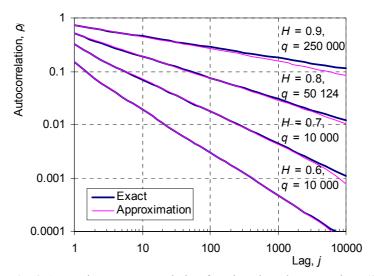
Fig. 9 Approximate autocorrelation functions based on equations (29) and (32) *vs* the exact autocorrelation functions of FGN for various values of the Hurst exponent *H* and the number of weights *q*.

Demonstration of the methods

The three proposed methods for generating FGN are demonstrated by synthesizing records with length, mean, variance and Hurst exponent equal to those of the historical standardized tree-ring series at Mammoth Creek, Utah. The generated synthetic record using the method of multiple time-scale fluctuation is plotted in Fig. 10. In comparison with the original series of Fig. 1(b) one can observe that this synthetic series exhibits a similar general shape with the same fluctuation amplitudes on all plotted time scales (1, 5 and 25 years). Figure 11 depicts the standard deviation of the aggregated processes $Z_i^{(k)}$ *vs* time scale *k* for this synthetic time series. The empirical curve is a straight line on the logarithmic plot with slope 0.75, i.e. equal to the assumed Hurst exponent. Figure 12 depicts the autocorrelation function of the
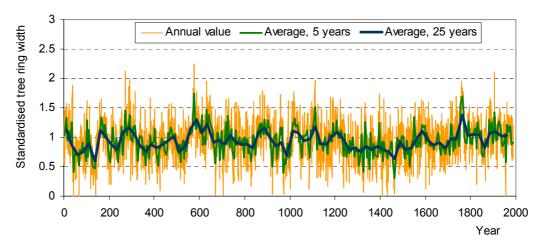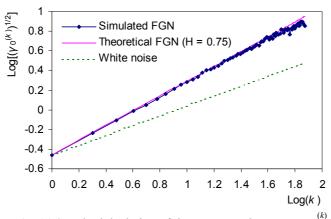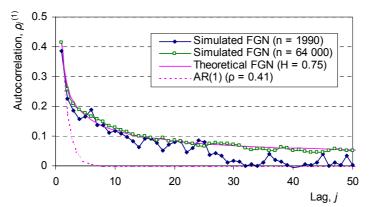

Fig. 10 Plot of a synthetic time series generated using the statistics of standardized tree rings at Mammoth Creek, Utah, and implementing: the multiple time-scale fluctuation approach.

Fig. 11 Standard deviation of the aggregated processes $Z_i^{(k)}$ *vs* time scale k (logarithmic plot) for the synthetic time series generated using the multiple time-scale fluctuation approach. For comparison the theoretical curves of the white noise and FGN models are also plotted.

Fig. 12 Autocorrelation function of the synthetic time series on the basic (annual) scale generated using the multiple time-scale fluctuation approach. For comparison the theoretical curves of the AR(1) and FGN models are also plotted as well as the empirical functions of an additional series with large length (64 000) generated using the same method.

same synthetic time series on the basic (annual) scale for lags up to 50. The empirical autocorrelation function is close to the theoretical one of FGN with $H = 0.75$. Some departures are due to sampling errors, as the record length of 1990 values is too small to accurately estimate autocorrelations for lags as high as 50. To verify this, an additional synthetic record was generated with 64 000 values and their auto-correlation functions were also plotted on Fig. 12. The empirical autocorrelation function of the latter series is almost indistinguishable from the theoretical one of the FGN process. The performance for the synthetic series generated using the other two methods—the disaggregation method and the symmetric moving average method—is similar (for legibility and brevity they are not shown in Figs 10–12, but may be found in Koutsoyiannis, 2002). In conclusion, this demonstration shows that all three methods are good for practical purposes.

CONCLUSIONS AND DISCUSSION

A first conclusion of this paper is that the Hurst phenomenon can be formulated and studied in an easy manner in terms of the variance and autocorrelation of a stochastic process on multiple time scales, thus avoiding the use of the complicated concept of rescaled range (see Appendix). In addition, the Hurst phenomenon may have a simple and easily understandable explanation based on the random fluctuation of a hydrological process upon different time scales. A second conclusion is that the generation of FGN, the process that reproduces the Hurst phenomenon, may be performed by one of three simple proposed methods that are based on (a) a multiple time-scale fluctuation approach, (b) a disaggregation approach, and (c) a symmetric moving average approach.

Of these three methods, (a) and (b) are very fast as the required computer time on a common PC is of the order of tens of milliseconds (for the applications presented here); this becomes of the order of seconds for method (c). Methods (b) and (c) can be directly extended to generate multivariate series as well (for a general framework of such adaptations for methods (b) and (c), see Koutsoyiannis, 2001 and 2000, respectively). Methods (a) and (c) can generate series with skewed distributions. Method (c) is the most accurate, but the other methods are sufficiently accurate and can be directly adapted to further improve accuracy, as discussed in the previous section. In general, all three methods are good for practical hydrological purposes. Method (a) may be preferable for single variate problems with symmetric or asymmetric distributions. Method (b) is best for single variate or multivariate problems with normal distribution. Finally, method (c) is good for any kind of problems, single variate or multivariate with symmetrical or asymmetric distributions, but it is slower than the other methods.

Obviously, FGN with its single parameter H is a simplified model of reality. Therefore, it may be not appropriate for all hydroclimatic series, even though it is much more consistent with reality, than the AR and ARMA process. A generalized and comprehensive family of processes, which can include a larger number of parameters and incorporates both the FGN and the ARMA processes, has been studied by Koutsoyiannis (2000).

REFERENCES

Bak, P. (1996) *How Nature Works, The Science of Self-Organized Criticality*. Copernicus, Springer-Verlag, New York, USA.

Beran, J. (1994) *Statistics for Long-Memory Processes*, vol. 61 of Monographs on Statistics and Applied Probability, Chapman and Hall, New York, USA.

Bhattacharya, R, N., Gupta, V. K. & Waymire, E. (1983) The Hurst effect under trends. *J. Appl. Prob.* **20**, 649–662.

Bloomfield, P. (1992) Trends in global temperature, *Climatic Change* **21**, 1–16.

Box, G. E. P., Jenkins, G. M. & Reinsel, G. C. (1994) *Time Series Analysis, Forecasting and Control.* Prentice Hall, Upper Saddle River, New Jersey, USA.

Bras, R. L. & Rodriguez-Iturbe, I. (1985) *Random Functions in Hydrology.* Addison-Wesley, Reading, Massachusetts, USA.

Ditlevsen, O. D. (1971) Extremes and first passage times. Doctoral dissertation, Technical University of Denmark, Lyngby, Denmark.

Eltahir, E. A. B. (1996) El Niño and the natural variability in the flow of the Nile River. *Wat. Resour. Res.* **32**(1), 131–137.

Evans, T. E. (1996) The effects of changes in the world hydrological cycle on availability of water resources. In: *Global Climate Change and Agricultural Production: Direct and Indirect Effects of Changing Hydrological, Pedological and Plant Physiological Processes* (ed. by F. Bazzaz & W. Sombroek), Chapter 2. FAO and John Wiley, Chichester, West Sussex, UK.

Graybill, D. A. (1990) IGBP PAGES/World Data Center for Paleoclimatology. NOAA/NGDC Paleoclimatology Program, Boulder, Colorado, USA.

Grygier, J. C. & Stedinger, J. R. (1990) SPIGOT, A synthetic streamflow generation software package, Version 2.5—technical description. School of Civil and Environmental Engineering, Cornell University, Ithaca, New York, USA.

Haan, C. T. (1977) *Statistical Methods in Hydrology.* Iowa State University Press, Ames, Iowa, USA.

Haslett, J. & Raftery, A. E. (1989) Space–time modelling with long-memory dependence: assessing Ireland's wind power resource. *Appl. Statist.* **38**(1), 1–50.

Hosking, J. R. M. (1981) Fractional differencing. *Biometrica* **68**, 165–176.

Hosking, J. R. M. (1984) Modeling persistence in hydrological time series using fractional differencing. *Wat. Resour. Res.* **20**(12), 1898–1908.

Hurst, H. E. (1951) Long term storage capacities of reservoirs. *Trans. ASCE* **116**, 776–808.

Klemeš, V. (1974) The Hurst phenomenon: a puzzle? *Wat. Resour. Res.* **10**(4), 675–688.

Kottegoda, N. T. (1980) *Stochastic Water Resources Technology.* Macmillan Press, London, UK.

Koutsoyiannis, D. (2000) A generalized mathematical framework for stochastic simulation and forecast of hydrologic time series. *Wat. Resour. Res.* **36**(6), 1519–1534.

Koutsoyiannis, D. (2001) Coupling stochastic models of different time scales. *Wat. Resour. Res.* **37**(2), 379–392.

Koutsoyiannis (2002) Internal report: http://www.itia.ntua.gr/getfile/511/2/2002HSJHurstSuppl.pdf.

Lane, W. L. & Frevert, D. K. (1990) *Applied Stochastic Techniques, User's Manual* (Personal Computer Version). Bureau of Reclamation, Engineering and Research Center, Denver, Colorado, USA.

Mandelbrot, B. B. (1965) Une classe de processus stochastiques homothétiques a soi: application à la loi climatologique de H. E. Hurst. *C. R. Acad. Sci. Paris* **260**, 3284–3277.

Mandelbrot, B. B. (1971) A fast fractional Gaussian noise generator. *Wat. Resour. Res.* **7**(3), 543–553.

Mandelbrot, B. B. (1977) *The Fractal Geometry of Nature*, 248. Freeman, New York, USA.

Mandelbrot, B. B. & Wallis, J. R. (1969a) Computer experiments with fractional Gaussian noises, Part 1: Averages and variances. *Wat. Resour. Res.* **5**(1), 228–241.

Mandelbrot, B. B. & Wallis, J. R. (1969b) Computer experiments with fractional Gaussian noises, Part 2: Rescaled ranges and spectra. *Wat. Resour. Res.* **5**(1), 242–259.

Mandelbrot, B. B. & Wallis, J. R. (1969c) Computer experiments with fractional Gaussian noises, Part 3: Mathematical appendix. *Wat. Resour. Res.* **5**(1), 260–267.

Mejia, J. M., Rodriguez-Iturbe, I. & Dawdy, D. R. (1972) Streamflow simulation, 2: The broken line process as a potential model for hydrologic simulation. *Wat. Resour. Res.* **8**(4), 931–941.

Mesa, O. J. & Poveda, G. (1993) The Hurst effect: the scale of fluctuation approach. *Wat. Resour. Res.* **29**(12), 3995–4002.

Montanari, A., Rosso, R. & Taqqu, M. S. (1997) Fractionally differenced ARIMA models applied to hydrologic time series. *Wat. Resour. Res.* **33**(5), 1035–1044.

National Research Council (Committee on Opportunities in the Hydrologic Sciences) (1991) *Opportunities in the Hydrologic Sciences*, 21. National Academy Press, Washington DC, USA.

Papoulis, A. (1991) *Probability, Random Variables, and Stochastic Processes* (third edn), 57. McGraw-Hill, New York, USA.

Radziejewski, M. & Kundzewicz, Z. W. (1997) Fractal analysis of flow of the river Warta. *J. Hydrol.* **200**, 280–294.

Salas, J. D. (1993) Analysis and modeling of hydrologic time series. In: *Handbook of Hydrology* (ed. by D. Maidment), 19.1–19.72. McGraw-Hill, New York, USA.

Salas, J. D. & Boes, D. C. (1980) Shifting level modelling of hydrologic time series. *Adv. Wat. Resour.* **3**, 59–63.

Salas, J. D., Delleur, J. W., Yevjevich, V. & Lane, W. L. (1980) *Applied Modeling of Hydrologic Time Series.* Water Resources Publications, Littleton, Colorado, USA.

Saupe, D. (1988) Algorithms for random fractals. In: *The Science of Fractal Images* (ed. by H.-O. Peitgen & D. Saupe), Chapter 2. Springer-Verlag, Berlin, Germany.

Stephenson, D. B., Pavan, V. & Bojariu, R. (2000) Is the North Atlantic Oscillation a random walk? *Int. J. Clim.* **20**, 1–18.

Toussoun, O. (1925) Mémoire sur l'histoire du Nil. In: *Mémoires a l'Institut d'Egypte*, vol. 18, 366–404.

Vanmarcke, E. (1983) *Random Fields*, 225. The MIT Press, Cambridge, Massachusetts, USA.

Vogel, R. M., Tsai, Y. & Limbrunner, J. F. (1998) The regional persistence and variability of annual streamflow in the United States. *Wat. Resour. Res.* **34**(12), 3445–3459.

Yevjevich, V. (1972) *Stochastic Processes in Hydrology.* Water Resources Publications, Fort Collins, Colorado, USA.

APPENDIX

Additional material related to the range concept

In hydrological texts, the Hurst phenomenon and related topics are analysed in terms of several storage-related families of random variables (e.g. Yevjevich, 1972; Kottegoda, 1980, p. 184; Salas, 1993, p. 19.14) like the partial sum:

$$Y_n := X_1 + X_2 + \ldots + X_n \tag{A1}$$

of the stochastic process X_i ($i = 1, 2, \ldots$), for any integer n; the range

$$R_n := \max(Y_i - i\,\mu; 1 \le i \le n) - \min(Y_i - i\mu; 1 \le i \le n) \tag{A2}$$

the adjusted range

$$R_n^* := \max(Y_i - i\,Y_n/n; 1 \le i \le n) - \min(Y_i - i\,Y_n/n; 1 \le i \le n) \tag{A3}$$

where the true mean μ has been replaced by the sample mean Y_n/n; and the rescaled range

$$R_n^{**} = R_n^* / S_n \tag{A4}$$

where S_n is the sample standard deviation of X_1, X_2, $\ldots$, X_n. The distributions of the random variables R_n, R_n^* and R_n^{**} depend on the distribution of X_i, the number n and the covariance structure of the process X_i; their determination is a very complicated task. Even their means are difficult to determine accurately (Yevjevich, 1972). For instance, in the simple case where X_i is an AR(1) Gaussian process with known μ and σ, the mean range is (Yevjevich, 1972, p. 158):

$$E[R_n] = \sigma \sqrt{\frac{2}{\pi(1-\rho^2)}} \sum_{i=1}^{n} \sqrt{\frac{1+\rho}{i(1-\rho)} - \frac{2\rho(1-\rho^2)}{i^2(1-\rho)^2}} \tag{A5}$$

(Interestingly, equation (A5) is displayed on the cover of the book by Yevjevich (1972).)

For R_n^* and R_n^{**}, only approximate relationships have been known. Generally, it is known that for all ARMA type processes, the rescaled range is asymptotically:

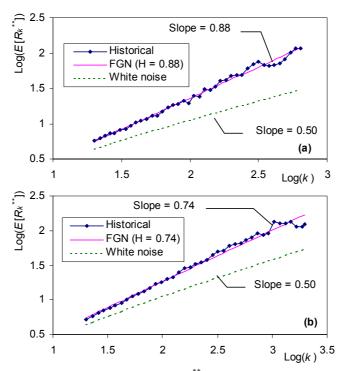$$E[R_n^{**}] \approx c\sqrt{n} \tag{A6}$$

and for the FGN process:

$$E[R_n^{**}] \approx c\,n^H \tag{A7}$$

where c is a constant (e.g. Bras & Rodriguez-Iturbe, 1985, p. 221).

Equation (A7) has been traditionally used to estimate the Hurst exponent. However, the uncertainty implied by equation (A7) is very high. It suffices to say that H can result in a value greater than one (for example, see Figs 7 and 8 in Vogel *et al.*, 1998), which is not allowed theoretically.

From a conceptual point of view, the range concept corresponds to the mass curve analysis of a reservoir (plot of cumulated inflows and outflows), a graphical method first developed by Ripple in 1883 and widely used in reservoir design since then. In this regard, R_n represents the required storage of a reservoir operating without any spill or other loss and providing a constant outflow equal to the mean flow. Obviously, this

Fig. A1 Mean rescaled range $E[R_k^{**}]$ *vs* time length k (logarithmic plots) for the two example historical data sets: (a) annual minimum water level of the River Nile; and (b) standardized tree rings at Mammoth Creek, Utah. For comparison approximate theoretical curves for the white noise and FGN models are also plotted.

is an oversimplification of a real reservoir. Therefore, this method needs to be abandoned today and the range concept needs to be replaced by probability-based design methods.

Because of the complications in definition and conceptualization of range indicators, the complex relationships of their statistical properties, and the estimation problems, their use has been avoided in this paper. It is shown that the concept of variance on multiple time scales is a much simpler and more accurate approach, which does not require the range concept at all. However, for the sake of compatibility with previous studies Fig. A1 is shown, in which the mean rescaled range R_n^{**} has been plotted as a function of length n for the two real-world example historical time series discussed earlier. It is observed that equation (A7) is validated with $H = 0.88$ for the Nile time series and $H = 0.74$ for the Utah time series. These values are close to the already estimated values, $H = 0.85$ and $H = 0.75$, respectively (Fig. 2).